2 receptor alpha chain (CD25) at a high level. We hypothesized that CD25 may be part of an active IL-2R signaling complex, allowing CLL cells to outcompete the CAR T cells for IL-2, limiting their activation and explaining the observed phenotype. We supplemented IL-2 into CLL/CAR T cell co-cultures which rescued the proliferative capacity of the CAR T cells and partially rescued cytokine production. Further, we performed intracellular cytokine staining of CAR T cells stimulated with aAPCs and CLL cells. Interestingly, we found that CLL cells fail to stimulate IL-2 production after either a 6- or 12-hour incubation, disproving the IL-2 sinking hypothesis. However, we did observe low-level CD107a acquisition, suggesting that the CAR T cells retain some cytotoxic function. We next proposed that low-level expression of co-stimulatory or adhesion molecules on CLL cells may impair CAR T cell activation. Immunophenotyping of the CLL cells showed low level expression of molecules such as CD54, CD80, and CD86. We hypothesized that up-regulation of these molecules could improve CAR T cell targeting of CLL cells. We activated CLL cells via CD40L and IL-4 which resulted in subsequent up-regulation of CD54, CD58, CD80, and CD86 as well as other molecules. Stimulation of CAR T cells with these activated CLLs enhanced CAR T cell proliferation and cell-conjugate formation, indicating stronger cell-to-cell interactions. Therefore, improving CLL stimulatory capacity can rescue T cell dysfunction. To assess whether IL-2 addition and CD40 ligation were synergistic, we combined the two assays; however, we saw no additional improvement over IL-2 addition alone. We showed that rescue via either IL-2 addition or CD40 ligation was not CAR-specific, as we observed similar defects and rescue with both a ROR1-targeting CAR and the gold standard CD19-targeting CAR. **Conclusions:**These data indicate that CAR T cell dysfunction in CLL is mediated by insufficient activation of CAR T cells rather than true defects in cell function. Improving the stimulatory capacity of CLL cells via IL-2 addition or CD40 activation may enable better clinical responses. Additionally, the requirement for enhanced co-stimulation and adhesion even in a second-generation CAR T cell containing a co-stimulatory signaling domain is a unique finding. Further, the conserved effect between CD19- and ROR1-targeting CARs suggests that these results may be broadly applicable to CAR T cell therapies, and may be relevant in other indications beyond CLL.

149. CAR Design and Expression Determine Hyper-Proliferative States in TET2 Deficient T Cells

Nayan Jain[1], Zeguo Zhao[1], Archana Iyer[1], Michael Lopez[1], Judith Feucht[2], Richard Koche[1], Julie Yang[1], Yingqian Zhan[1], Michel Sadelain[1]

[1] Memorial Sloan Kettering Cancer Center, New York, NY,[2]University of Tübingen, Tübingen, Germany

TET2 disruption through a chance integration of a 4-1BB chimeric antigen receptor (CAR) lentiviral vector led to the emergence of a dominant CAR T cell clone, which coincided with tumor clearance in a chronic lymphocytic leukemia (CLL) patient (Fraietta et. al. Nature 2018). The enhanced proliferative ability ascribed to the *TET2* disruption opened the possibility of treating patients with lower doses of TET2 deficient CAR T cells than are currently required. In a pre-clinical murine model of human acute lymphoblastic leukemia (ALL), we studied the effect of CAR design in determining the effect of *TET2* editing on T cell phenotype and anti-tumor efficacy. To assess the effect of *TET2* disruption on CAR T cell therapeutic efficacy, we treated immune deficient mice bearing the human ALL cell line, NALM6, with limiting doses of either *TET2* edited (CRISPR/Cas9) or unedited CAR T cells. We investigated the two most widely used second generation CD19-specific CARs encompassing the costimulatory domain of either CD28 (Rv-1928z) or 4-1BB (Rv-19BBz). *TET2* editing enhanced the anti-tumor efficacy of Rv-19BBz CAR T cells and promoted the acquisition of a central memory phenotype. In contrast, *TET2* editing did not alter the anti-tumor efficacy of Rv-1928z CAR T cells or their differentiation state. As Rv-1928z CAR T cells have a stronger induction of effector differentiation than Rv-19BBz CAR T cells, this divergence led us to hypothesize that *TET2* editing acts in concert with CAR signaling to remodel the T cell phenotype. To test this hypothesis, we edited *TET2* in two additional CAR designs that have been shown to limit T cell effector differentiation over retrovirally encoded CD28 costimulated CARs: 1928z driven by the *TRAC* promoter (*TRAC*-1928z) and Rv-1928z co-expressing the 4-1BB ligand (Rv-1928z-41BBL). Indeed, disruption of *TET2* enhanced the anti-tumor efficacy of both these CAR T cells and increased their early central memory phenotype. However, *TET2* edited CAR T cells, over time, attain a hyper-proliferative phenotype with a near total loss of effector function. This state was consistently associated with biallelic *TET2* editing. The frequency with which *TET2* edited T cells achieved hyper-proliferation depended on the signaling properties of the CAR receptor. This hyper-proliferative state is associated with sustained upregulation of cell cycle factors and shares features with some T cell leukemia/lymphoma. Exome analysis identified point mutations and chromosomal aberrations in hyper-proliferative cells, but they were not conserved across different populations, suggesting an alternate mechanism as a likely candidate for driving the hyper-proliferation. Chromatin accessibility analysis revealed that loss of *TET2* sets an epigenetic state that allows for sustained elevated levels of BATF3, which in turn drives a MYC-dependent proliferative program in *TET2* deficient CAR T cells. Our study shows that disruption of *TET2* may enhance the proliferation and persistence of T cells, depending on their CAR receptor, but that *TET2* deficient CAR T cells eventually uncouple their proliferative program from effector function thus impairing their therapeutic potency.

150. Tumor-Responsive, Multifunctional CARNK Cells Cooperate with Impaired Autophagy to Infiltrate and Target Glioblastoma

Jiao Wang[2], Sandro Matosevic[1,2]

[2] Department of Industrial and Physical Pharmacy, Purdue University, West Lafayette, IN,[2]Center for Cancer Research, Purdue University, West Lafayette, IN

Background: Tumor antigen heterogeneity, a severely immunosuppressive tumor microenvironment (TME), and

suppression of NK cell function: tumor-associated proteases (TAP) mediated site-specific release of anti-CD73 scFv which can inhibit the activity of CD73 independently of CAR signaling and decrease the local concentration of adenosine (**Fig.1A-C**). To address insufficient homing of NK cells into the tumor bed, we combined these cells with chloroquine (CQ) as an adjuvant to inhibit autophagy in GBM and evaluated these cells against patient-derived intracranial GBM models in vivo (**Fig.1D**). **Results:** When administered with CQ, CD73.mCARpNK cells could effectively target orthotopic patient-derived GBM xenografts, demonstrating effective anti-tumor responses (**Fig.1E** and **F**), potent inhibition of CD73 expression (**Fig.1G** and **H**) and remarkable suppression of adenosine production in the local tumor (**Fig.1I** and **J**). In addition, we also unveiled a complex reorganization of the immunological profile of GBM induced by inhibiting autophagy. In particular, pharmacologic impairment of the autophagic process promoted a significant secretion of chemokines, including CCL5 and CXCL10, which were favorable to NK cell infiltration (**Fig.1K**). In response to combination therapy with CD73.mCAR-pNK cells and CQ, we detected significantly elevated presence of NK cells in GBM tumors in brains of treated mice, which correlated to higher chemokine levels (**Fig.1L** and **M**). **Conclusions:** We built a novel, sophisticated combinatorial platform for GBM: a multifunctional immunotherapy based on genetically-engineered, human NK cells bearing multiple antitumor functions, including local tumor responsiveness, that addresses, for the first time, key drivers of GBM resistance to therapy: antigen escape, immunometabolic reprogramming of immune responses, and poor immune cell homing. **References** [1] Pombo Antunes AR, Scheyltjens I, Duerinck J, Neyns B, Movahedi K, Van Ginderachter JA. Understanding the glioblastoma immune microenvironment as basis for the development of new immunotherapeutic strategies. Elife. 2020;9:e52176.

Cardiovascular and Pulmonary Gene Therapy

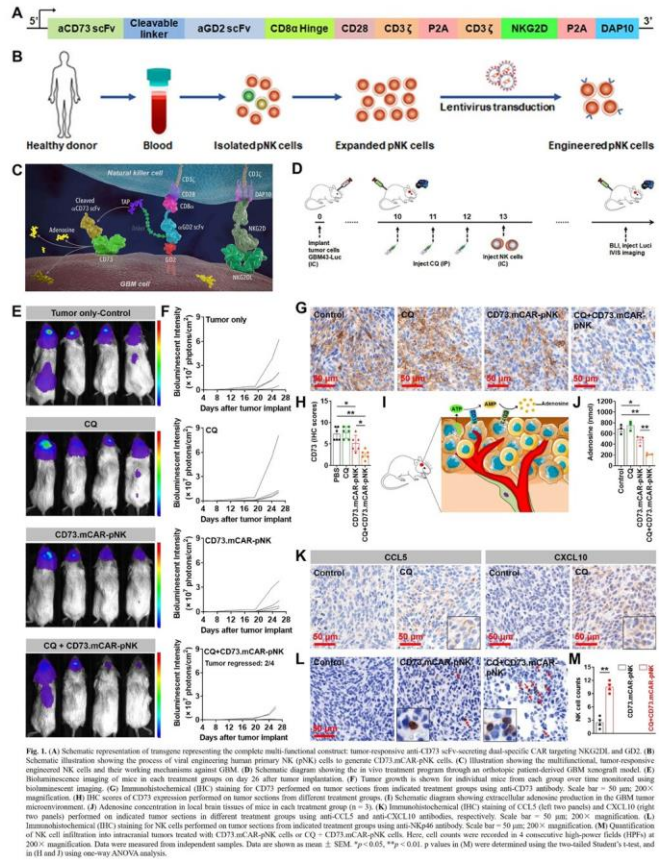

Fig. 1. (**A**) Schematic representation of transgene representing the complete multi-functional construct: tumor-responsive anti-CD73 scFv-secreting dual-specific CAR targeting NKG2DL and GD2. (**B**) Schematic illustration showing the process of viral engineering human primary NK (pNK) cells to generate CD73.mCAR-pNK cells. (**C**) Illustration showing the multifunctional, tumor-responsive engineered NK cells and their working mechanisms against GBM. (**D**) Schematic diagram showing the in vivo treatment program through an orthotopic patient-derived GBM xenograft model. (**E**) Bioluminescence imaging of mice in each treatment groups on day 26 after tumor implantation. (**F**) Tumor growth is shown for individual mice from each group over time monitored using bioluminescent imaging. (**G**) Immunohistochemical (IHC) staining for CD73 performed on tumor sections from indicated treatment groups using anti-CD73 antibody. Scale bar = 50 μm; 200× magnification. (**H**) IHC scores of CD73 expression performed on tumor sections from different treatment groups. (**I**) Schematic diagram showing extracellular adenosine production in the GBM tumor microenvironment. (**J**) Adenosine concentration in local brain tissues of mice in each treatment group (n = 3). (**K**) Immunohistochemical (IHC) staining of CCL5 (left two panels) and CXCL10 (right two panels) performed on indicated tumor sections in different treatment groups using anti-CCL5 and anti-CXCL10 antibodies, respectively. Scale bar = 50 μm; 200× magnification. (**L**) Immunohistochemical (IHC) staining for NK cells performed on tumor sections from indicated treatment groups using anti-NKp46 antibody. Scale bar = 50 μm; 200× magnification. (**M**) Quantification of NK cell infiltration into intracranial tumors treated with CD73.mCAR-pNK cells or CQ + CD73.mCAR-pNK cells. Here, cell counts were recorded in 4 consecutive high-power fields (HPFs) at 200× magnification. Data were measured from independent samples. Data are shown as mean ± SEM. *$p < 0.05$, **$p < 0.01$. p values in (M) were determined using the two-tailed Student's t-test, and in (H and J) using one-way ANOVA analysis.

151. ADCLEC.syn1 Is a Novel Combinatorial CAR Platform for Enhanced Therapeutic Index in AML

Sascha Haubner, Jorge Mansilla-Soto, Sarah Nataraj, Jae Park, Xiuyan Wang, Isabelle Rivière, Michel Sadelain

Center for Cell Engineering and Immunology Program, Memorial Sloan Kettering Cancer Center, New York, NY

Relapsed/refractory (r/r) AML is associated with very poor prognosis. The only curative option to date is allogeneic stem cell transplantation which is limited due to high treatment-related toxicity and therapeutic failure, creating a high medical need for potent yet tolerable novel therapies. CAR therapy has high potential for successful application beyond CD19-positive B cell malignancies, however suitable CAR targets in AML still need to be identified. Integrating proteomic and transcriptomic target expression data we have previously discovered n=24 CAR candidate targets with a favorable profile in AML and normal tissues and provided a rationale for several combinatorial CAR approaches in AML (Perna et al. Cancer Cell 2017). We have further validated

lymphopenia resulting in inadequate immune intratumoral trafficking all contribute to glioblastoma (GBM) being highly resistant to therapy [1]. Though intratumoral presence of NK cells is beneficial to GBM patients, current GBM immunotherapies have struggled to overcome these challenges and demonstrate sustained clinical improvements in patient overall survival (OS). As a result, new immunotherapeutic approaches for this deadly cancer that are able to address all three of these critical hurdles are needed. **Methods:** We generated multifunctional human NK (CD73.mCAR-pNK) cells that express a dual-specific CAR redirected against ligands for NKG2D and GBM-associated GD2 receptors, and a third functional moiety that can be activated in the GBM TME to address immunometabolic

favorable target pairs among our 24 candidates, based on a multimodal in-depth analysis including multiparameter spectral flow cytometry of primary r/r AML and normal bone marrow samples, along with normal tissue immunohistochemistry studies and mass-spectrometry. We focus here on ADGRE2 and CLEC12A, two cell surface molecules highly co-expressed in AML but with largely non-overlapping expression profiles in normal tissues. We hypothesized that rational combinatorial CAR design targeting both ADGRE2 and CLEC12A enhances anti-leukemic efficacy without cumulating potential on-target/off-tumor toxicity. Using a bicistronic gamma-retroviral vector, we screened different combinatorial CAR formats targeting ADGRE2 and CLEC12A. Specific to the combined target expression profile in malignant versus normal cells, we fine-tuned both scFv affinities considering total avidity, eventually achieving thresholds for mediating cytolysis in the context of optimized CD3 zeta signaling. In addition, we further optimized the chimeric receptor combination by evaluating different hinge/ transmembrane and costimulatory domains. To provide a platform for identification of the ideal combinatorial CAR design, we established in-vitro and in-vivo models based on a human AML cell line with up- or down-regulated antigen levels of ADGRE2 and CLEC12A to mimic both AML antigen-low escape and toxicity to normal cells. Ultimately, using therapeutically relevant T cell doses we were able to identify a combinatorial CAR format that allowed complete and durable AML remission across relevant target levels while sparing cell line clones representing normal cells.

Cardiovascular and Pulmonary Gene Therapy

152. Systemic *Hps1* Gene Augmentation Prevents Pulmonary Manifestations in a Mouse Model of Hermansky-Pudlak Syndrome

Shachar Abudi[1,2], Marina Zieger[3], John D. Burke[1], Lisa J. Garrett[4], Yair Anikster[2,5], Bernadette R. Gochuico[1], William A. Gahl[1,6], Christian Mueller[3], May C. Malicdan[1,6]

[1]Human Biochemical Genetics Section, NHGRI, NIH, Bethesda, MD,[2]Tel Aviv University, Tel Aviv, Israel,[3]Horae Gene Therapy Center, University of Massachusetts Medical School, Worcester, MA,[4]Transgenic Mouse Core, NHGRI,
NIH, Bethesda, MD,[5]Sheba Medical Center, Ramat Gan, Israel,[6]NIH UDP, NHGRI, NIH, Bethesda, MD

Mutations in *HPS1* cause Hermansky-Pudlak syndrome type 1 (HPS1), an autosomal recessive disorder manifesting with oculocutaneous albinism, a bleeding diathesis, and a highly penetrant and lethal form of pulmonary fibrosis (HPSPF). A prominent finding in the lungs of HPSPF patients is the presence of enlarged and foamy type II alveolar cells (AECII), which are thought to have critical roles in alveolar homeostasis. Alteration in the function of AECII cells have been shown to promote dysregulated repair and pathogenic activation of fibroblasts, ultimately leading to fibrosis. There is no FDA-approved treatment for HPSPF; the identification of effective therapy has been hindered by the lack of preclinical models that represent the human HPS genotype and phenotype. Because *HPS1* mutations are lossof-function, we hypothesized that introduction of a normal copy of *HPS1* could be a strategy for treatment. With the goal to establish gene therapy for HPS-1, we systemically administered adeno-associated virus (AAV) harboring the open reading frame of the murine *Hps1* to a novel *Hps1* knockout mouse that we generated.We deleted *Hps1* in mice by using CRISPR-Cas9 ($Hps1^{delta/delta}$). These mice recapitulated human HPS-1 phenotypes, and presented with enlarged and foamy AECII, increased susceptibility to bleomycin-induced PF, reduced pigmentation, and a bleeding diathesis. Molecularly these mice show no *Hps1* mRNA expression in their lungs and other tissues. To determine which AAV serotype is suited to target AECII, we injected AAV5 or AAV8 harboring GFP to one-day old via the facial vein. We performed *in situ* hybridization of RNA, immunohistochemistry of GFP protein and molecular quantification. Our results reveal that AAV5 and AAV8-GFP are highly expressed in lung cells, including AECII, after 1 month of augmentation.For *in vivo* gene augmentation, we injected systemically AAV5 or AAV8 harboring murine *Hps1* to one-day old mice. Phenotypic characterization included molecular analysis, examination of lung pathology, and measurement of lung physiology. Six months after gene augmentation mice given AAV5Hps1 or AAV8-Hps1 revealed an increase of about 80% in *Hps1* mRNA in their lungs compared to lungs of untreated mice that did not express *Hps1* mRNA. More importantly, histological analysis showed improvement of the lung phenotype including reduction in the size and number of enlarged and foamy AECII (Figure 1), which correlated with higher *Hps1* expression. Taken altogether, our results show that gene augmentation of AAV can prevent the pulmonary manifestations in our *Hps1* knockout mouse and can be used in designing therapeutic options for HPSPF.

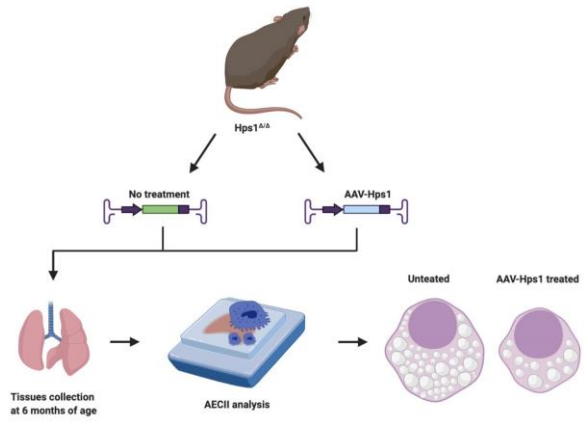

Figure 1. Schematic presentation of approach to gene augmentation.
AAV5 or AAV8 encoding *Hps1* were injected into $Hps1^{delta/delta}$ mice. Tissues were collected and analyzed after 6 months. Lung histology of $Hps1^{delta/delta}$ untreated mice reveals enlarged and foamy type II alveolar epithelial cells (AECII). Mice that were transduced with AAV5 or AAV8 *Hps1* had smaller and less foamy AECII.

153. Generation of a Human 3D Lung Model for Therapeutic Gene Editing in Surfactant Protein B Deficiency

Helena C. M. Meyer-Berg, Stephen C. Hyde, Deborah R. Gill

Radcliffe Department of Medicine, University of Oxford, Oxford, United Kingdom

Surfactant protein B (SP-B) deficiency is a rare autosomal recessive disease of the lung leading to severe respiratory distress that is fatal within the first months of life. Conventional therapies such as steroids or surfactant replacement therapy are ineffective in these individuals. Gene therapy has the potential to treat SP-B deficiency by restoring surfactant homeostasis. Cross-species variation can hamper gene therapy development, because of variable expression of viral entry receptors crucial for (e.g. rAAV) vector entry. Moreover, genomic differences complicate testing of targeted gene editing tools in non-human models. We established a human model of SP-B deficiency to address these complications, choosing a human 3D-lung model generated from the human embryonic stem cell line RUES2. These lung bud organoids (LBOs), described by Chen and colleagues [Nat Cell Biol, (2017) 19: 542], exhibit a bias towards generation of lung parenchyma, especially surfactant-producing ATII cells. We previously used this model to screen rAAV serotypes suitable for transduction of the human parenchyma and identified rAAV6.2 as a promising candidate, concluding that LBOs are a suitable lung gene therapy model [Stem Cell Res Ther 2020 11: 448]. To grow SP-B deficient LBOs, RUES2 embryonic stem cells were gene edited to achieve the 121ins2 (C > GAA) mutation in SFTPB - the most common mutation in SP-B deficiency (ca. 66% of cases). HDR gene editing was performed by electroporation of Cas9 RNP (Synthego) and ssDNA donor. Because of the low efficiency of HDR editing, electroporation was first optimised. The highest levels of HDR gene editing were achieved using the CA137 electroporation programme (Lonza), with up to 89 % indel formation and 59 % knock-in achieved as determined by ICE analysis. After cloning and screening of 58 clones, 53 % were identified as 121ins2 edited via restriction fragment length polymorphism analysis. Next, 14 RUES2 121ins2-edited clonal lines were confirmed by Sanger sequencing reactions, twice after isolation and twice during clonal expansion. Two clones were taken forward for further characterisation. A normal karyotype was confirmed for both via KaryoStat microarray and the retention of stem cell status was examined for both lines by immunocytochemistry for markers SOX2, OCT4, TRA-1-60 and SSEA4. LBOs were grown from the parental line and from one of the 121ins2 edited clones. Firstly, endoderm was induced and induction efficiency determined by flow cytometry. The parental cell line and the edited clone were 90.2 % and 90.5 % double positive for the endoderm markers CXCR4 and c-Kit, respectively. During anterior foregut endoderm induction, expression of FOXA2 was confirmed at similar levels in both cell lines with immunocytochemistry. Finally, lung progenitor organoids were placed in Matrigel for maturation and branching. The morphology was documented over the entire organoid generation and at no point were differences between cell lines observed. Buds developed within 2 weeks, with similar budding efficiency observed. On day 77 of maturation, Western blot analysis indicated expression of SP-B in the wild-type organoids and its absence in the 121ins2 edited LBOs. In summary, we have generated a human embryonic stem cell line to model the SP-B deficient lung, with opportunity to screen for gene therapies or therapeutic gene editing strategies, in an effort to accelerate translational research.

Cardiovascular and Pulmonary Gene Therapy

154. Vectored Immunoprophylaxis for COVID-19 (COVIP)

Yue Du[1], Kamran Miah[1], Habib Omar[1], Helena Meyer-Berg[1], YanQun Wang[2], JinCun Zhao[2], Stephen Hyde[1], Deborah Deborah[1]

[1]Nuffield Department of Clinical Laboratory Sciences, Radcliffe Department of Medicine, University of Oxford, Oxford, United Kingdom,[2]State Key Laboratory of Respiratory Disease, Guangzhou Institute of Respiratory Health, the First Affiliated Hospital, Guangzhou, China

A quest for effective therapeutics and prophylactic strategies for COVID-19 pandemic is still an active pursuit. Protein-based therapeutics, such as monoclonal antibodies (mAbs) that target epitopes on the SARS-CoV-2 Spike (S) protein represent a novel approach, but such therapeutics typically have short half-lives, necessitating repeated delivery. A more promising strategy against SARS-CoV-2 infections is to use vector-mediated immunoprophylaxis (VIP) by directing the sustained production of neutralising mAb into serum or in a localized fashion. Among multiple recombinant viral vectors, our preferred vector is based on a third-generation, selfinactivating simian immunodeficiency virus (rSIV) pseudotyped with the Fusion and Haemaglutinin-Neuraminidase surface glycoproteins from Sendai virus (rSIV.F/HN), which directed a sustained expression of broadly neutralising mAb to confer completely protection against supra-lethal influenza infection (Tan 2020 Thorax 2020;75:1112). As a comparison, we also included recombinant Adeno-associated virus (rAAV) vector 9 and 8 serotypes, which are gold standard to offer VIP against pathogens of importance.Since the laboratory BALB/c mice are not naturally susceptible to Coronavirus, we provided human ACE2 (hACE2) in trans via rAAV9 vector to facilitate SARS-CoV-2 pseudovirus (encoding luciferases; S-LV.luciferase) entry in lungs. Intranasal (IN) delivery of S-LV to the hACE2-expressing mice resulted in dose-dependent luciferase expression, which peaked at peaked at 7 days post-delivery (8.72E4±4.14E4 p/s/cm2/sr, Average Activity Radiance). Ultimately, we utilised hACE2-expressing murine model and S-LV as a means to investigate a novel VIP for COVID-19 (COVIP) strategy.The sequence for anti-SARS-CoV-2 monoclonal antibody (mAb) NC0321, isolated from the PBMCs of a COVID-19 convalescent patient, was inserted into the rSIV.F/HN.hCEF, rAAV. hCEFI and rAAV.CASI vectors. To test prophylaxis, 1e11 GC AAV9 or 5e8 TU rSIV.F/HN mAb vector were co-administrated in a single IN administration with 1e11 GC rAAV9.hACE2; 1e11 GC of rAAV9 mAb vector was delivered by intramuscular injection and followed by an IN delivery of rAAV9.hACE2 under the same anaesthesia conditions. The NC0321 IgG expression level was increased from day 7 to day 14, reaching a plateau at day 14 onwards. At day 28 post-delivery, IgG expression level was about 0.5,1 and 5 μg/ml for rSIV.F/HN, rAAV9, and

rAAV8 vectors expressing NC0321, respectively. In all three cases, NC0321 IgG expression in sera was significantly higher than that in naïve mice (****, *p<0.001*). At 28 days post-delivery, the IgG expression level in the mouse epithelial lining fluid was about 5, 50 and 20 μg/ml for rSIV.F/HN, rAAV9, and rAAV8 vectors expressing NC0321, respectively. Encouragingly, on maximal challenge with S-LV. luc to hACE2-expressing mice, luciferase expression was significantly reduced in mice intranasally dosed with rSIV.F/HN and rAAV9 vector expressing NC0321 compared with an isotype control (**, *p=0011* or *0.0052*, respectively; AUC of the average luminescence). Interestingly, rAAV8-mediated expression of NC0321 conferred no significant protection.Here we compare different vector platforms and delivery routes for SARS-CoV-2 specific antibody gene transfer based on a hACE2 murine model. Our study indicates that vector delivery of mAb by direct lung inhalation route is efficient to confer protection against SARS-CoV-2 mimic. This COVIP strategy may offer protective immunity for vulnerable individuals unable to mount an effective immunological response for COVID-19.

155. Impact of Transplant Immunosuppression on In Vivo Lung-Selective CRISPR/Cas9 Therapeutics for Lung Transplantation

Kumi Mesaki, Stephen Juvet, Zehong Guan, Jim Hu, Alan Davidson, Marcelo Cypel, Mingyao Liu, Shaf Keshavjee

University Health Network, Toronto, ON, Canada

Background: Donor lung gene modification using CRISPR/Cas9 holds promise in lung transplantation (LTx). Immunologic enhancement of donor lungs by epigenetic or genetic modification using CRISPR/Cas9 could address the shortage of donor organs, improve outcomes, and eventually eliminate the need for life-long systemic immunosuppression. For CRISPR/Cas9 therapeutics to modulate a whole donor organ, efficient delivery is critical to achieve the therapeutic effects. Adenoviral vectors provide high efficacy with rapid expression and have sufficient capacity to deliver the Cas9 and guide RNAs (gRNAs) in a single package. Nonetheless, adenoviruses are known to have significant immunogenicity, particularly in the lung - an organ vulnerable to inflammation and injury. Consequently, expression of transgenes after adenoviral delivery is transient. Further, Cas9 is itself immunogenic, thus creating an additional potential barrier to clinical translation of CRISPR/Cas9 therapeutics with adenoviral vectors. Anti-rejection immunosuppression required in LTx can be utilized to minimize vector-related inflammation. Furthermore, viral delivery to the organ ex vivo, prior to host exposure to the graft further facilitates this process. This has made the possibility of gene therapy more promising. We therefore hypothesized that the use of transplant immunosuppression could permit effective CRISPR/Cas9 therapeutics in vivo in the lung. **Methods**: Adenovirus expressing a Cas9 activator (dSaCas9VPR) was trans-bronchially delivered to Lewis rats at a high dose (2.5E8 PFU/rat). The effect of standard triple immunosuppression (methylprednisolone, cyclosporine, and azathioprine) with or without additional methylprednisolone on vector-related inflammation was assessed in four groups (Fig A, B) after 72 hours. Next, to elucidate the impact of immunosuppression on the persistence of epigenome editing, adenovirus expressing Cas9 activator and gRNAs was delivered to activate the IL-10 gene at low dose (1E8 PFU/rat), and assessed after day 14 with or without daily immunosuppression. **Results**: Delivery of high dose adenovirus expressing Cas9 activator without immunosuppression (Group 1) worsened oxygenation and lung edema: PaO2 (435±55 vs 674±20, p<0.0001), wet/dry ratio (5.63±0.33 vs 4.59±0.14, p=0.0013) compared to the diluent group (Group 4, Fig C, D). Triple immunosuppression (Group 2) improved oxygenation compared to the no immunosuppression group (Group 1). Additional steroid administration (Group 3) further improved the condition of the lung leading to PaO2 (610±38, p=0.35) and wet/dry (4.77±0.48, p>0.99) ratios comparable to the diluent (control) group (Group 4). Adenovirus expressing two gRNAs induced IL-10 gene expression with minimal inflammation at low dose, as shown by a significantly increased IL-10/IL-6 protein ratio in the lung (Fig E). Daily immunosuppression sustained IL-10 gene activation until day 14 (relative expression; 32.3±6.5 vs 0.67±0.14, p<0.0001, Fig F) as well as Cas9-expression and viral DNA, suggesting immunosuppression inhibited elimination of the transduced cells. **Conclusion**: Transplant immunosuppression ameliorates inflammation and prolongs the effect of CRISPR/Cas9 epigenome editing with adenovirus in the lung. This study illustrates a strategy for effective gene editing by managing vector-related inflammation in an in vivo CRISPR/Cas9 therapeutics.

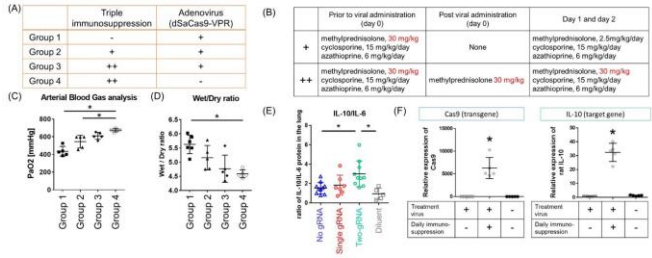

156. First Proof-of-Concept of miQURE™ Based Gene Targeting in the Liver: Lipid Lowering and Atherosclerosis Suppression by AAV-miQURE™-Mediated ANGPTL3 Targeting

Vanessa Zancanella[1], Astrid Valles-Sanchez[1], Carlos Vendrell Tornero[1], Maroeska Oudshoorn-Dickmann[1], Hendrina Wattimury[1], Kristel van Rooijen[1], Mark van Veen[1], Monika Golinska[1], Elsbet J. Pieterman[2], Nanda Keijzer[2], Hans M. G. Princen[2], Geurt Stokman[2], Martin de Haan[1], Ying Poi Liu[1]

[1]uniQure Biopharma B.V., Amsterdam, Netherlands,[2]TNO Metabolic Health Research, Leiden, Netherlands

We have developed a proprietary, next-generation miQURE™ technology, where a transcript encoding artificial microRNAs (miRNAs) is packaged into adeno-associated viral (AAV) vectors for mRNA silencing. Our AAV5-miQURE™ targeting mutant huntingtin in the brain is currently being tested in a phase 1/2a clinical study in Huntington Disease patients. In the current study, we have used Dyslipidemia as indication to investigate the potency of AAV-based miQURE™ to lower Angiopoietin-like 3 (ANGPTL3) in the liver. ANGPTL3 loss-of-function genetic variants have been associated with low levels of plasma

triglycerides, low-density lipoprotein cholesterol, and high-density lipoprotein cholesterol, and a decreased risk of cardiovascular diseases. Pharmacological inhibition of ANGPTL3 mimics the phenotype of individuals carrying mutations impairing ANGPTL3 and lowers plasma lipids in mice, monkeys and humans. After *in vitro* testing, the most promising miQURE™ candidates were tested for their efficacy to lower ANGPTL3 mRNA and ANGPTL3 plasma levels in wild-type and transgenic mice with a humanized lipoprotein metabolism (APOE*3-Leiden.CETP). The lead candidate resulted in wild-type mice in a dose-dependent decrease in ANGPTL3 mRNA expression (up to ~77%) and a subsequent up to ~90% reduction

Cardiovascular and Pulmonary Gene Therapy

in ANGPTL3 plasma levels. APOE*3-Leiden.CETP mice received AAV-miANGPTL3 treatment with or without the standard of care treatment, statin (atorvastatin). AAV5-miANGPTL3 delivery to the liver resulted in a significant and sustained reduction in triglycerides and plasma total cholesterol, whereas the levels in the vehicle and control scrambled miRNA groups remained unchanged. Furthermore, a significant decrease in total atherosclerotic lesion area could be observed in the AAV-miANGPTL3 treated group (58% compared to scrambled miRNA). Treatment with AAV-miANGPTL3 was associated with maintenance of an non-diseased plaque phenotype and reduction in the lesion severity. A further reduction in total cholesterol and triglycerides exposure and in the total atherosclerotic lesion area was observed in the combination treatment with atorvastatin. To provide proof of concept of liver directed miANGPTL3 expression, a non-human primates study was conducted. In this study, the animals received a high caloric diet to induce hyperlipidemia. Similar to the mouse study, the main goal was to assess miRNA, mRNA and relevant plasma lipid markers. The AAV-miANGTPL3 treatment was welltolerated in all animals during the in-life phase of 22 weeks. However, the individual animal response on the high calory diet varied greatly, resulting in variable data. Nevertheless, preliminary results suggest that the AAV5-miANGTPL3 group showed a slight lowering in total cholesterol and triglycerides. In conclusion, we here report the first proof-of-concept of a miQURE™-based approach in the liver. The combination of tolerability of miQURE ™ expressed in the liver of non-human primates and proof-of-concept in mice supports the continuation of its development for liver-directed indications and translation in the clinic.

157. Abstract Withdrawn

Clinical Trials and Advanced Preclinical Studies for Neurologic Diseases

158. Electroporation Mediated Gene Transfer of MRCKα to the Lungs of Mice Effectively Treats Pre-Existing Acute Lung Injury

Jing N. Liu[1], Michael Barravecchia[2], David A. Dean[2]

[1]The Cellular and Molecular Pharmacology and Physiology, University of Rochester School of Medicine and Dentistry, Rochester, NY,[2]Pediatrics, University of Rochester School of Medicine and Dentistry, Rochester, NY

Acute Lung Injury (ALI) and its more severe form Acute Respiratory Distress Syndrome (ARDS) are severe conditions characterized by alveolar fluid accumulation and insufficient gas exchange, ultimately leading to acute respiratory failure. Both impaired alveolar fluid clearance (AFC) and a disrupted alveolar-capillary barrier contribute to the pathogenesis of ALI/ARDS. Most attempts at therapy in the past have focused on enhancing AFC, but repairing the alveolarcapillary barrier is likely also needed for effective treatment. We previously have shown that overexpression of the β1 subunit of the Na^+, K^+-ATPase (β1- Na^+, K^+-ATPase) increases AFC in lungs of multiple species. We also have found that electroporation-mediated gene delivery of the β1- Na^+, K^+-ATPase rescues lipopolysaccharide (LPS) induced ALI by upregulating tight junction (TJ) proteins and pulmonary barrier function, demonstrated by decreased lung permeability, total protein and cellularity in bronchoalveolar lavage (BAL) fluid, and improved overall outcome of lung injury. While studying how the β1- Na^+, K^+-ATPase increases lung barrier, we identified MRCKα (CDC42 binding protein kinase alpha) as an interacting partner of the β1 subunit. Previous data from our lab indicate that MRCKα mediated β1's upregulation of TJ proteins and epithelial barrier integrity in cultured cells. However, it is unknown whether MRCKα can upregulate pulmonary barrier function and treat LPS induced ALI *in vivo*. Understanding this question would help to determine the therapeutic potential of MRCKα for ARDS. Plasmids expressing MRCKα or β1- Na^+, K^+-ATPase were delivered individually or in combination by aspiration and transthoracic electroporation to mice which had been pre-injured by LPS intratracheal administration 24 hours earlier. Two days after gene delivery, various endpoint assays were performed to evaluate lung edema, permeability, inflammation and histological injury. We found that overexpression of MRCKα alone attenuated LPSincreased edema, lung leakage, BAL cellularity and protein concentration, restored TJ protein expression, and improved overall outcome of lung injury, similar to gene transfer of the β1- Na^+, K^+ATPase. However, we found that unlike β1- Na^+, K^+-ATPase, gene transfer of MRCKα alone did not enhance AFC. These results indicate that MRCKα could benefit the pre-injured lungs by reducing pulmonary edema, restoring lung barrier function and reducing inflammation. Moreover, they also suggest that improving barrier function alone may be of equal or

even more benefit than improving AFC in order to treat ALI/ARDS. (Supported by: NIH grants HL120521, HL131143, and HL138538 and an AHA predoctoral fellowship (JL))

Clinical Trials and Advanced Preclinical Studies for Neurologic Diseases

159. Gene Therapy Candidate for Metachromatic Leukodystrophy (MLD):

Summary of Preclinical *In Vivo* Data Following an Intravenous Delivery of HMI-202

Jacinthe Gingras, Thia St-Martin, Katie Gall, Tania A. Seabrook, Jason Lotterhand, Israel Rivas, Nancy Avila, Michael Mercaldi, Jennifer Newman, Shiva Krupa, Teresa Wright, Omar Francone, Albert Seymour
Homology Medicines Inc, Bedford, MA

Metachromatic leukodystrophy (MLD) is an inherited autosomal recessive lysosomal storage disorder (LSD) with a great unmet medical need. This fatal neurodegenerative LSD occurs in three forms: late infantile (prevalence of 1 in 40,000), juvenile, and adult. The late infantile and juvenile forms represent the majority of the MLD patients where mortality at 5 years is estimated at 75% and 30%, respectively. MLD is most commonly caused by mutations in the *ARSA* gene and patients suffering from the disease are deficient in arylsulfatase-A (ARSA) enzyme activity. The disease is characterized by accumulation of sulfatides to supraphysiologic and toxic levels in the peripheral organs and nervous system. In the brain, excess sulfatides lead to the destruction of myelin, a key protective layer of the nerve fibers that enhances propagation of action potentials. Herein, we report preclinical gene therapy data where a single intravenous (IV) dose of HMI-202 (AAVHSC15-human-*ARSA* (h*ARSA*)) crosses the blood-nerve- and blood-brain-barriers (BNB and BBB) in juvenile non-human primates (NHP) and in the *Arsa* KO murine model of MLD. In the HMI-202treated adult *Arsa* KO mice, hARSA expression patterns are nearly identical to that of murine Arsa (mArsa) distribution in the nervous system of wild type age-matched littermates, in both neuronal and glial cellular profiles. In HMI-202-treated adult *Arsa* KO mice, we show a dose-response relationship in hARSA enzyme activity, transcript, and vector genomes in the central nervous system (CNS). As early as 1 week following administration (earliest time-point of collection), near-normal human adult levels of hARSA activity are detected in the CNS of HMI-202-treated adult *Arsa* KO mice, and levels are sustained at or above normal adult human brain levels throughout the study (52 weeks post-dose). Similarly, hARSA enzyme activity is detected 1 week post-dose in the CNS of *Arsa* KO neonates and is sustained out to 12 weeks post-dose (end of study). Furthermore, we demonstrate modulatation of key biochemical markers in the CNS, including murine neuronal sulfatides, myelin and lymphocyte (MAL) transcript, lysosomal-associated membrane protein-1 (LAMP-1), and glial fibrillary acidic protein (GFAP) levels in HMI-202-treated *Arsa* KO mice. Lastly, using the rotarod assay, we demonstrate a functional motor benefit in HMI-202-treated *Arsa* KO mice dosed prior to the detectable accumulation of CNS neuronal sulfatides (~2 months of age). In summary, a single-IV dose of HMI-202 crossed the BNB and BBB in lower (mice) and higher (NHP) species. In addition, the ability to achieve hARSA enzyme activity levels at or above normal human adult brain levels, rapid onset of expression, durability, broad biodistribution, modulation of key biomarkers, and functional motor benefit in a murine MLD disease model was demonstrated. These preclinical data from IND-enabling studies continue to support the further optimization and development of HMI-202 as a gene therapy for the treatment of MLD.

160. Gene Replacement Therapy for Angelman Syndrome

Justin Percival, Kasturi Sengupta, Long Le, Khalid Arhzaouy, Heather Born, Elizabeth Buza, Cecilia Dyer, James M. Wilson
Gene Therapy Program, University of Pennsylvania, Philadelphia, PA

Angelman syndrome (AS) is a rare neurodevelopmental disorder affecting approximately half a million individuals worldwide. AS is characterized by intellectual and physical disability, seizures, impaired sleep, and gut dysfunction. Many of these deficits result from a loss of the maternally inherited ubiquitin protein ligase E3A (*UBE3A*) allele. At present, therapeutic options for AS are limited. Adeno-associated virus (AAV)-based gene replacement therapy represents a promising strategy for restoring *UBE3A* isoform expression and mitigating AS severity. However, the *UBE3A* gene encodes three isoforms, and it is currently unclear which *UBE3A* isoform is the most effective candidate. We addressed this uncertainty by comparing the efficacy of AAV vectors delivering codon-optimized human *UBE3A* isoforms in a mouse model of AS. Western blotting and immunohistochemical analyses indicated that intracerebroventricular injections of AAV-UBE3A human isoform 1 and 2 vectors into neonatal control and AS mice resulted in robust protein expression. Isoform 1 replacement significantly improved gait, nest-building ability, and motor coordination in a dose-dependent manner in AS mice. In contrast to isoform 1, isoform 2 further impaired nest-building ability and motor coordination in AS mice. Ongoing toxicology studies in nonhuman primates suggest that a high dose of AAV-UBE3A isoform 1 vector injected into the cisterna magna has no significant adverse effects. Taken together, these data indicate that the AAV-UBE3A isoform 1 vector is the most therapeutically effective option with a promising safety profile. These preclinical findings represent an important step forward in the development of gene replacement therapy for AS.

161. An AAV-miRNA for Androgen Receptor Knockdown in Spinal and Bulbar Muscular Atrophy

Eileen Workman, Julia Johansson, Mariya Kostiv, Christian Hinderer, James M. Wilson
Gene Therapy Program, University of Pennsylvania, Philadelphia, PA

Introduction: Spinal and bulbar muscular atrophy (SBMA) is an X-linked, slowly progressive motor neuron disease caused by a polyglutamine (CAG) expansion tract within exon 1 of the androgen receptor (AR). The expansion results in the nuclear aggregation of the

AR protein, which then causes motor neuron degeneration almost exclusively in males due to androgen-mediated activation of toxicity. To date, no effective treatment has been approved for SBMA. Since knockdown of the androgen receptor in neurons does not appear to cause adverse effects, lowering AR levels in SBMA is an attractive strategy for treating the disease. Our gene therapy approach involves delivering an AAV vector expressing an miRNA targeting the AR to motor neurons. **Results:** We screened for artificial miRNAs

targeting the AR in cell culture and identified a candidate miRNA. Artificial miRNAs were cloned into a miR-155 backbone with a cytomegalovirus promoter and transfected into HEK293 cells. Using qPCR and Western blot analysis, we identified an AR-targeting candidate miRNA, GTP-miR001, which shares homology in mouse, human, and rhesus macaque. GTP-miR001 was able to knock down up to 60% of AR expression in HEK293 cells. The candidate miRNA was packaged into an AAV. PHP.eB vector for *in vivo* testing in wild-type C57BL/6J mice. It was determined that IV injection of AAV.PHP.eB.GTP-miR001 at 3e11 was sufficient to achieve greater than 50% knockdown of the androgen receptor in the mouse brain and 70% knockdown in the spinal cord. To evaluate the potential efficacy of GTP-miR001 for the treatment of SBMA, we tested an AAV serotype hu68 vector expressing the miRNA in AR97Q SBMA transgenic mice. These mice express high levels of the human AR with a pathogenic repeat expansion and display a very severe SBMA phenotype with progressive hindlimb weakness that ultimately results in death. Males have a median survival of 91 days and females have a median survival of 184 days. Intravenous administration of the AAVhu68.GTP-miR001 vector in 3- or 5-week-old mice resulted in efficient knockdown of the AR, with modest improvements in survival and motor phenotype that correlated with the degree of AR suppression. Treating AR97Q mice as neonates yielded robust improvements in weight gain, motor phenotype, and survival, indicating the necessity of early intervention in this rapidly progressive mouse model. **Conclusions:** We have identified a candidate AAV vector expressing an artificial miRNA for the treatment of SBMA. This vector was capable of knocking down AR protein expression *in vitro* and *in vivo*. Further, we were able to achieve improvement of the phenotype and survival of AR97Q SBMA transgenic mice when subjects were injected at the neonatal stage. Ongoing studies include the determination of vector toxicity and knockdown of AR protein in nonhuman primates.

162. AXO-AAV-GM1 for the Treatment of GM1 Gangliosidosis: Preliminary Results from a Phase I-II Trial

Cynthia J. Tifft[1], Precilla D'Souza[1], Jean Johnston[1], Maria Acosta[1], Caroline Rothermel[1], Audrey Thurm[2], Ajith Karunakara[3], Benjamin Thorp[3], Peter Ross[3], John Jameson[3], Toby Vaughn[3], Donna Valencia[3], Erika De Boever[3], Gavin Corcoran[3]

[1]Office of the Clinical Director, NHGRI, National Institutes of Health, Bethesda, MD,[2]National Institute of Mental Health, National Institutes of Health, Bethesda, MD,[3]Sio Gene Therapies, New York, NY

GM1 gangliosidosis is a rare, inherited neurodegenerative disorder caused by mutations in the *GLB1* gene which encodes the lysosomal hydrolase β-galactosidase (β-gal). The resulting enzyme deficiency leads to a toxic accumulation of GM1 ganglioside, predominantly in the central nervous system (CNS) where its rate of synthesis is the highest, but also in peripheral tissues. GM1 gangliosidosis is uniformly fatal, and there are no disease-modifying treatments currently available. As this is a monogenic disorder, it is an ideal target for gene therapy to deliver β-gal to the CNS and periphery, with resulting potential to halt further neurodegeneration, restore function and ameliorate symptoms. This is a preliminary analysis from an ongoing open-label, single-arm, Phase I-II trial (ClinTrials.gov, NCT03952637) in which subjects with a confirmed genetic and biochemical diagnosis of GM1 gangliosidosis were treated with AXO-AAV-GM1 (AAV9-GLB1), an investigational gene therapy utilizing an adeno-associated virus (AAV9) vector to deliver a functional copy of the *GLB1* gene. All subjects received 1.5 $x10^{13}$ vg/kg of AXO-AAV-GM1 administered via intravenous infusion and immune modulation with rituximab, sirolimus and glucocorticoids. The primary endpoint of the trial is safety/tolerability, secondary efficacy endpoints include Vineland-3, brain MRI, motor function and disease severity. Biomarkers of disease progression or stabilization (βgal activity and GM1 ganglioside in serum and CSF) are also assessed. Six-month follow-up data are presented from 4 subjects with the late infantile (Type IIa) form and one with juvenile (Type IIb) disease. AXO-AAV-GM1 was generally safe and well-tolerated and there have been no serious adverse events (SAEs) related to gene therapy. One SAE was described: a single subject experienced bacterial sepsis due to a PICC line infection, which was considered to be unrelated to the investigational product, and which resolved following line removal and administration of IV antibiotics. The most common adverse events were considered mild to moderate. Four subjects had AST elevations that were considered to be adverse events. None required clinical intervention or had associated clinical sequelae. There were no other adverse events indicative of impaired liver function including serum bilirubin, GGT, and ALT. Serum β-gal enzyme activity was sampled at 9 distinct post-baseline timepoints between Day 7 and Month 6. The mean increase from baseline ranged from 71-138% across the 9 time points. At Month 6, serum enzyme activity was sustained with an increase from baseline ranging from 33%-128% across the 5 subjects. Subjects were assessed by multiple measures of neurodevelopment including the Vineland Adaptive Behavior Scales 3rd Edition (VABS-3), Upright and Floor Mobility Score, and Clinical Global Impression (CGI). All 5 subjects demonstrated disease stability at 6 months post-treatment as assessed by VABS-3 Growth Scale Value scores, Upright and Floor Mobility Score, and CGI relative to baseline values. Per protocol, brain MRIs were not collected for the 6-month follow-up analysis but will be completed at later timepoints. We will continue to follow-up these subjects and are now evaluating additional subjects receiving 4.5 $x10^{13}$ vg/kg dose of AXO-AAV-GM1.

163. AXO-Lenti-PD Gene Therapy for Parkinson's Disease: Efficacy, Safety, and Tolerability Data from the Second Cohort in Open-Label Dose Evaluation Study SUNRISE-PD at 6 Months Post Administration

Gavin Corcoran[1], Ajith Karunakara[1], Ben Vaughn[2], Elimor Brand-Schieber[1], Thomas Foltynie[3], Roger A. Barker[4], Stéphane Palfi[5]

[1]Sio Gene Therapies Inc., New York, NY,[2]Rho Inc., Durham, NC,[3]Department of Clinical and Movement Neurosciences, UCL Institute of Neurology, London,

United Kingdom,[4]John van Geest Centre for Brain Repair, Department of Clinical
Neuroscience, Addenbrooke's Hospital, Cambridge, United Kingdom,[5]AP-HP, Groupe Hospitalier Henri-Mondor, DMU CARE, Neurochirurgie, Créteil, France

AXO-Lenti-PD (ALPD, previously known as OXB-102), a novel gene therapy for Parkinson's disease (PD), uses a lentiviral vector to deliver the three genes required for endogenous dopamine synthesis (TH, CH1 and AADC), into the putamen with the goal of improving motor fluctuations and long term quality of life. In the Phase I/II study OXB102-01 (SUNRISE-PD; NCT03720418), six subjects were dosed with ALPD: Cohort1 (n=2; Low dose, 4.2E+6 Transducing Units [TU]) and Cohort2 (n=4; Mid dose, 1.4E+7 TU). Efficacy data reported here are from Cohort1 and Cohort2 6-month visits (6M). Given the small sample size, only descriptive statistics were planned. Two of four subjects did not have UPDRS "OFF" 6M data recorded: one due to COVID-19 site limitations and the other declined the OFF assessment. The two evaluable subjects in Cohort 2 had 20.5-point (40%) improvement from baseline (BL) in UPDRS III (Motor Examination) 'OFF'. UPDRS Part II (Activities of Daily Living) "OFF" had 13.5-point improvement (71%). Subjects used the Hauser home diary for up to 3 consecutive days within the week prior to the study visit to log their motor function (either Asleep, ON without dyskinesia, ON with nontroublesome dyskinesia, ON with troublesome dyskinesia, or OFF) at 30 minute intervals normalized to 16 waking hours. Good ON time (the sum of ON without dyskinesia and ON with non-troublesome dyskinesia) increased from BL by 2.2 hours (h) across the four Cohort2 subjects at 6M, while OFF time decreased by 2.3h. Levodopa equivalent daily dose (LEDD) decreased 271.0 mg, 13% lower than at BL. Table 1 summarizes individual and mean changes.

Table 1 Change from Baseline

Subject	OFF Time (h)	Good ON Time (h)	LEDD (mg)	UPDRS II OFF	UPDRS III OFF
Cohort 1					
1001	+2.8	-2.4	-98	-26	-20
1003	-0.5	+2	-150	-13	-14
Mean	**+1.2**	**-0.2**	**-124 (11%)**	**-19.5 (65%)**	**-17.0 (29%)**
Cohort 2					
2002	-0.6	+0.6	0	-12	-22
2004	-0.2	+0.1	-700	-	-
2006	-3.9	+3.5	-466	-	-
2007	-4.6	+4.5	+81	-15	-19
Mean	**-2.3**	**+2.2**	**-271 (13%)**	**-13.5 (71%)**	**-20.5 (40%)**

A total of four serious adverse events (SAEs), all unrelated to ALPD and resolved, have been reported: Parkinson's disease (ie, worsening of non-motor OFF related to anxiety) and Major depression in a Cohort1 subject; Confusional state and Wound infection in a Cohort2 subject. No hypersensitivity, immune or endotoxicity related adverse events have been reported. No serious unexpected suspected adverse reactions (SUSARs) have been reported. No subject died or discontinued from the study. The 6M data from the first two cohorts in SUNRISE-PD trial showed that ALPD gene therapy was generally well tolerated, and the initial efficacy data suggest the potential for a clinically relevant effect. Further evaluation of ALPD is planned using a higher dose/volume open label cohort followed by sham-controlled study.

164. Safety Evaluation of IV-Administered BBP-812, an AAV9-Based Gene Therapy for the Treatment of Canavan Disease, in Mice and Juvenile Cynomolgus Macaques

David W. Scott, Jeremy Rouse, Kirsten Romero, Rachel Eclov, Mayank Kapadia, Daniel McCoy, Clayton W. Beard
Aspa Therapeutics, Raleigh, NC

Canavan Disease (CD) is a rare pediatric leukodystrophy caused by aspartoacylase deficiency. The disease is characterized by elevated levels of the aspartoacylase substrate N-acetylaspartic acid and patients present with a lack of psychomotor development with an average lifespan of less than ten years. We are developing BBP-812, an AAV9-based gene therapy containing a codon modified human *Aspa* transgene, to introduce functional aspartoacylase into CD patients. Proof of concept studies in Aspa -/- mice demonstrated that intravenous (IV) dosing of BBP-812 could reverse signs and symptoms of CD. To better understand the safety of IV delivered BBP-812, we conducted studies in non-human primates (NHP; juvenile cynomolgus macaques) and a GLP-toxicology study in C57Bl/6 mice. The NHP study included IV doses of $3.14x10^{13}$, $1.05x10^{14}$, and $3.14x10^{14}$ vg/ kg with animals sacrificed three and eight weeks after dosing. In the mouse study, animals were dosed at $1.0x10^{14}$, and $3.0x10^{14}$ vg/kg and

were sacrificed four, twelve, and twenty-four weeks after dosing. Safety readouts for both studies included clinical chemistry and hematology, immunology, and microscopic evaluation of major organs systems. For the NHP study, the microscopic evaluation of the nervous system included four spinal cord regions and eight dorsal root ganglia (DRG) per animal. Key findings in the NHP study were a transient increase in ALT and AST in the highest dose IV treatment group at day 3 which returned to normal without intervention by day 8. No other changes in hematology or clinical chemistry occurred during the study. Immunological analysis revealed that all treated animals developed antibodies to AAV9 and the majority of animals developed antibodies to Aspa after dosing. There were no adverse test article-related microscopic changes in the study at any dose level at either necropsy timepoint. Test article-related changes were observed only in the liver (portal infiltrates and/or increased cellularity) in some of the $3.14x10^{14}$ vg/kg treated animals. These findings were considered minor, did not impact the clinical health of the animals, and were not associated with any tissues damage. Evaluation of the spinal cord and DRG revealed sporadic minimal findings that were also present in control animals. Importantly, there

was no evidence of axonopathy in the spinal cord or DRGs as has been reported with other AAV9-based therapies. In the GLP-toxicology study in mice there were no adverse test article related changes in any clinical chemistry or hematology during the study. Creatine kinase and lactate dehydrogenase were decreased at both dose levels at all timepoints but this was not considered adverse. Immunological analysis revealed that all BBP-812 treated animals generated antibodies to AAV9 while no animals generated antibodies against Aspa. T-cells were monitored for reactivity to AAV9 and Aspa. There was a minor response in some animals to AAV9 with no response detected towards Aspa. There were no microscopic changes in the study in any group at any time point. Based on these findings, the NOAEL from the NHP study was determined to be $3.14x10^{14}$ vg/kg and from the GLP toxicology study in mice was determined to be $3.0x10^{14}$ vg/ kg of IV-administered BBP-812. These studies support the continued development of BBP-812 for the treatment of CD.

165. Gene Replacement Therapy for *SURF1*-Related Leigh Syndrome Using AAV9

Qinglan Ling, Matthew Rioux, Steven Gray
UTSW, Dallas, TX

SURF1(surfeit locus protein 1)-related Leigh syndrome (LS) (also known as Charcot Marie Tooth disease type 4K) is an early onset neurodegenerative disorder characterized by reduction in the assembly factor of complex IV, resulting in disrupted mitochondrial function. Here, we hypothesized that functional gene replacement strategy could restore mitochondrial functions in LS caused by *SURF1* loss-offunction mutations. A codon-optimized version of the human *SURF1* (h*SURF1*) packaged within self-complementary adeno-associated virus serotype 9 (AAV9) viral vectors (AAV9/h*SURF1*), which have been shown to induce robust expression in central nervous system (CNS), was designed and generated as the treatment entity. Our and other studies indicated that the knockout (KO) of *SURF1* in mice reduced complex IV/cytochrome *c* oxidase (COX) activity and MT-CO1 (mitochondrially encoded cytochrome *c* oxidase I) protein expression in multiple organs, as well as induced lactic acidosis. Thus, we treated juvenile *SURF1* KO mice with AAV9/h*SURF1* through broad CNS-

directed delivery (intrathecal (IT) administration, or a combination of intrathecal and intravenous administration), in a manner that is compatible with human translation. Our data indicate that 4 weeks after intrathecal administration into juvenile mice, the COX activity was partially and significantly rescued in all tissues tested, including liver, brain and muscle. Furthermore, our histology study suggest AAV9/ h*SURF1*-treated mice showed dose-dependently increased h*SURF1* mRNA expression and restoration of MT-CO1 protein expression in the brain, which further supported our findings in COX activity. Additionally, we tested endurance capacity and lactic acidosis 4 weeks and 9 months after the treatment in a separate group of mice. Our data suggest that the gene replacement treatment also mitigated the lactic acidosis upon exhaustive exercise at mid-age. However, doubling the total amount of virus by administering through both intravenous and intrathecal route did not confer any significant improvement compared to an intrathecal route alone in any of the parameters tested above, except the COX activity in liver. This suggests a single dose IT administration of AAV9/h*SURF1* is effective and sufficient in improving SURF1 deficiency-related dysfunctions. The toxicity of the vectors was evaluated through intrathecal administrating into wildtype (WT) mice at a maximum feasible dose. There were no toxicities observed in either the in-life portion of the study or after microscopic examination of major tissues up to a year following gene transfer. Taken together, we propose gene replacement therapy through IT administration of AAV9/ h*SURF1* as a potential treatment worthy of further development for *SURF1*-related LS patients. Further, this general approach might be amenable as a potential treatment for patients with other related forms of LS or other mitochondrial disorders.

Downstream Process of Vector Manufacturing

166. Novel Platform for Transport and Delivery of Recombinant Adeno-Associated Virus without Need for Cold Storage during Transit

Maria A. Croyle[1,2,3], Trang Doan[1], Matthew D. Le[1], Irnela Bajrovic[1,4], Lorne Celentano[4], Charles Krause[4], Haley G. Balyan[4], Abbie Svancarek[4], Lakmini Wasala[4], Angela Mote[4], Anna Tretiakova[4], R. Jude Samulski[3,4]
[1]College of Pharmacy, University of Texas at Austin, Austin, TX,[2]John R. LaMontagne Center for Infectious Disease, Austin, TX,[3]Jurata Thin Film, Chapel Hill, NC,[4]AskBio, Research Triangle Park, NC

Within the past 30 years, significant progress has been made in the development of gene vectors with several therapies receiving approval by the European Medicines Agency (EMA) and the U.S. Food and Drug Administration (FDA). Despite this progress, these products are stored and shipped at $\leq$ -70°C, similar to current COVID19 vaccines. This poses significant logistic and economic issues with respect to global distribution and access to life-saving medicines. In an effort to address these important issues, we developed a novel method for stabilizing live viruses in a peelable thin film matrix that can be stored at ambient temperature (see figure). In these studies, an AAV9 vector (AAV9-CBALuc) was mixed with film base formulation, poured into 1 ml molds and dried under aseptic conditions. Films were peeled and packaged in individual particle free-bags with foil overlays and stored at room temperature under controlled humidity. A sublot of films were shipped from Texas to North Carolina via overnight courier in an envelope without ice or cold blocks for in vivo testing. Control preparations were stored in a commercial liquid formulation at room temperature and 4 and -80 °C for comparison. Over 95% of the original infectious dose of AAV was recovered after drying as determined by *in vitro* transduction assays measuring transgene expression and internalized viral genome copies. In contrast, infectious virus particles could not be detected in the liquid formulation after 30 days at room temperature with large aggregates detected by dynamic light scattering at 14 days transitioning to